6. Numerical modelling of deformation changes induced by lake-level fluctuations of the Hohenwarte reservoir, Thuringia, Germany

Abstract[a]

The Hohenwarte reservoir in southeast Thuringia (Germany) is a medium-sized artificial reservoir, holding on average 180 Mill. m^3 of water. It was constructed between 1936 - 43 and is operational since then. The water load impounded induces stress and deformations of the underlying crust and upper mantle.
The Geodynamic Observatory Moxa is located around 4 km to the north. The observatory is equipped with seismometers and sensitive tilt– and strainmeters, accurate to the nrad and nstrain range.
We explore the deformation effects caused by the water load of the Hohenwarte reservoir, both on a short-term seasonal time scale and a long-term decadal time scale. The seasonal effect, mainly induced by elastic deformation, results in tilt and strain deformation in the 4 μrad and 1 μstrain ranges, respectively. Long-term decadal variations, however, are unlikely to be significant, if a realistic viscoelastic structure of the underlying upper mantle is used.

[a] Steffen and Kaufmann (2006a). Numerical modelling of deformation changes induced by lake-level fluctuations of the Hohenwarte reservoir, Thuringia, Germany, J. Geodyn. 41(4), 411 - 421; Steffen and Kaufmann (2006b). Influence of the Hohenwarte reservoir on tilt and strain observations at Moxa. Bull. d'Inf. Mar. Terr. 142, 11399 - 11406.

6.1 Introduction

Artificial reservoirs hold back water behind a concrete or earthen dam. They are important for flood protection, for providing drinking water and for the generation of electricity. Furthermore, many jobs can be provided around a reservoir, especially in the tourism business. From a scientific view, the filling of reservoirs with water induces a load on the Earth's surface, deforming the crust and mantle and producing tilt and strain deformations. In addition, reservoir-induced deformations due to accumulation of large water masses behind a dam are potentially seismogenic [e. g. Rothe, 1968; Simpson, 1976; Withers, 1977; Bell et al., 1978; Li and Han, 1987].

The deformation of the Earth's surface by reservoirs has been studied extensively in the literature. Some examples are discussed below:

Lambert et al. [1986] observed an anomalous relative vertical uplift of 4 cm and relative changes in gravity of 14 μgal after the filling of La Grande-2 reservoir, Quebec, Canada. The gravity change is thought to be the result of lateral transport of water in a high-permeability formerly undersaturated zone, hydraulically coupled to the reservoir. The possible elastic expansion of cracks and fractures in this zone or unexpectedly high rates of regional tilting cause the anomalous uplift.

Kaufmann & Amelung [2000] investigated the reservoir-induced deformation in vicinity of Lake Mead, Nevada, USA, to constrain the rheological properties of the continental crust and of the uppermost mantle. The reservoir has a total volume of 35.5 km^3 and encompasses an area of 635 km^2. The subsidence pattern clearly showed relaxation of the underlying basement due to the water load of the lake.

Wang [2000] calculated the water load-induced surface vertical displacements and level plane changes in the front reservoir area of the Three-Gorges Reservoir, China, during the filling period and discussed the height changes. The results are thought to bound the water load-induced responses. For the expected water level of 175 m, a maximum depression of 48.3 mm was derived.

A first stage of subsidence monitoring for Salto Caxias power dam in Brazil was summarised by Santos et al. [2001]. Here, a monitoring network to determine the subsidence of the surrounding area to be flooded was implemented before closing of the dam. By stage 1 the network design, installation and first field campaign is meant, so no results are derived yet.

Yan et al. [2004] reported that the Jiangya dam, China, and the rock masses on both valley sides were uplifted to various degrees during the filling of the reservoir, with a measured maximum uplift of 32.6 and 19.08 mm, respectively. To understand the uplift mechanism, a 3D numerical analysis was carried out. The authors concluded that the rise of an artesian head of a confined hot aquifer as a result of the reservoir inundation is the principal factor contributing to the uplift.

The Hohenwarte reservoir in the southeast of Thuringia is the 3rd largest reservoir in Germany with a volume of 182 Mill. m^3, covering an area of 7.3 km^2. In 4 km distance to the reservoir, the Geodynamic Observatory Moxa is situated. The data of seismometers and strainmeters are successfully used for studies of the Earth's interior structure and properties. With the used types of instruments it is possible to observe tilt changes in the range of 10^{-9} rad and displacement changes of 10^{-9} strain. We explore the possibility that registrations of the seismometers and strainmeters are influenced by deformation changes induced by lake-level fluctuations of the Hohenwarte reservoir. We therefore use the Finite Element (FE) method to calculate the deformations in vicinity of the Hohenwarte reservoir.

6.2 Saale Kaskaden

In the southeast of Thuringia, the river Saale crosses the Thuringian Slate Mountains between Blankenberg and Saalfeld (Fig. 6.1). The drop in elevation on a length of 80 km is about 170 m. Till the 1920's the Saale was running through small and deep valleys. Due to the small, incised valley, the spring snowmelt often resulted in floods. Three large flood catastrophes, in November 1890, February 1909 and January 1918, were the reason for planning several artificial dams, the Saale Kaskaden (Fig. 6.1). They should catch the water of the Saale and its tributary Wisenta in several reservoirs. The first reservoir was the Wisenta reservoir, dammed by a 60 m long barrage and finished in 1920. Later on, between 1933 to 1934 this barrage was replaced by a concrete dam. The two largest reservoirs, the Bleiloch reservoir and the Hohenwarte reservoir were built between 1926 to 1932 and between 1936 to 1943, respectively. In 37 years a new landscape along the Saale was formed. All reservoirs with their dimensions are summarised in Tab. 6.1.

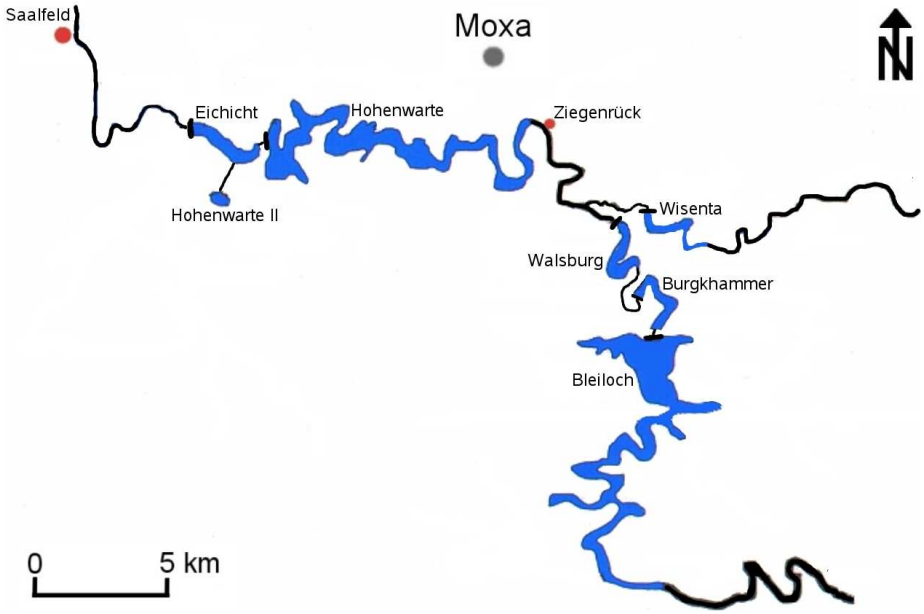

Figure 6.1: Overview of the Saale Kaskaden with the seven reservoirs and the artificial dams (black bars) between Blankenberg and Saalfeld.

The Hohenwarte reservoir is the 3rd largest reservoir in Germany. The lake encompasses an area of 7.3 km^2, and the total volume is 182 Mill. m^3. The dam was built between 1936 and 1943, and put into operation in 1941. The balance reservoir is the 4.3 km long Eichicht reservoir in the west. The task of the Hohenwarte reservoir is generation of electricity, flood protection and increasing the base flow of the rivers Elbe and Saale in the summer months.

6.3 Geodynamic Observatory Moxa

The Geodynamic Observatory Moxa, a station of the German Regional Seismic Network (GRSN), is located about 30 km south of Jena (Thuringia, Germany) at the border of the Thuringian Slate Mountains

Table 6.1: Reservoir dimensions of the Saale Kaskaden.

name	construction	volume in 10^6 m^3	length in km	area in km^2	concrete dam l [m] x h [m]
Wisenta	1933 - 1934	1.04	2.4	0.28	148 x 16
Bleiloch	1926 - 1932	215.00	28.0	9.20	205 x 65
Burgkhammer	1930 - 1932	5.64	6.5	0.84	122 x 22
Walsburg	1938 - 1939	2.54	5.0	0.50	118 x 16
Hohenwarte	1936 - 1943	182.00	27.0	7.30	412 x 75
Eichicht	1942 - 1945	5.21	4.3	0.71	215 x 20
Hohenwarte II	1956 - 1963	3.28	-	0.22	man-made basin

(Fig. 6.1) and is maintained by the Institute of Geosciences of the Friedrich–Schiller University Jena. It is embedded on the east hill flank of the remote Silberleite valley. The seismometers and two quartz tube strainmeters are installed in a gallery between 20 and 50 m deep in a hill. The covering with rock and gravel is about 35 m. The strainmeters have a length of 26 m with one instrument installed in EW– and NS–direction, respectively. The rock in the observatory area is dominated by metapelite. The distance from the observatory to the Hohenwarte reservoir is about 4 km. For further information, a detailed description of the observatory can be found in Teupser [1975] and Jahr et al. [2001].

6.4 Model description

6.4.1 Geometry

We model the water impounded in the Hohenwarte reservoir as surface load on a flat, viscoelastic earth by means of the FE method. We employ the modelling software ABAQUS [Hibbitt et al., 2005].

The earth model is a cube with 100 km side length and consists of 13 layers in vertical direction, simulating the crust and the upper mantle. Looking on the surface, the generated mesh of $100 \times 100 \times 13$ hexahedra elements is divided into a centre and a peripheral frame. The 20 km $\times$ 20 km large centre, between 40 and 60 km in each horizontal direction, is meshed with 80×80 elements with a horizontal side length of 250 m. The remaining 10 element rows of the 40 km wide peripheral frame have a variable side length from short side lengths near the centre to long side lengths for the outer elements. With 25 m, the elements in the first layer have the smallest thickness in vertical direction. The second layer has a thickness of 225 m, layers 3 to 5 a thickness of 250 m. The other thickness values for layers 6 to 13 are summarised in Tab. 6.2. The material parameters for the crust and the upper mantle are taken from PREM [Dziewonski and Anderson, 1981, Tab. 6.2]. The depth of the Mohorovičić discontinuity at the Hohenwarte reservoir location is, after Dèzes & Ziegler [2001], around 29 ± 1 km. To simplify the geometry of the model, the transition between crust and upper mantle is set to 25 km. A linear, elastic

Table 6.2: Model dimensions and parameterisation.

layer	thickness in m	depth in km	density in kg/m^3	Young's modulus in GPa	Poisson's ratio	
1	25	0.025	2600	67.9	0.282	
2	225	0.25	2600	67.9	0.282	
3	250	0.5	2600	67.9	0.282	
4	250	0.75	2600	67.9	0.282	crust
5	250	1	2600	67.9	0.282	
6	1000	2	2600	67.9	0.282	
7	8000	10	2600	67.9	0.282	
8	15000	25	2913	111.6	0.263	
9	15000	40	3380	173.3	0.280	
10	15000	55	3378	172.8	0.280	
11	15000	70	3377	172.3	0.280	upper mantle
12	15000	85	3375	169.5	0.283	
13	15000	100	3373	165.9	0.287	

rheology is used for the crust and for model 1 also for the upper mantle (Fig. 6.2). Thus, model 1 simulates a purely elastic Earth. A viscoelastic rheology for the upper mantle is used for two calculations: in model 2, the viscosity for the upper mantle is set to 5×10^{20} Pa s, and in model 3 to 10^{19} Pa s between 25 and 40 km and 5×10^{20} Pa s below. Thus, models 2 and 3 allow the relaxation of stress in the upper mantle. The viscosity of 5×10^{20} Pa s for the upper mantle in model 2 is taken as an average of upper-mantle viscosities beneath Europe resolved by different investigations in the last years [see Steffen and Kaufmann, 2005, for a summary]. The viscosity of 10^{19} Pa s for the uppermost mantle in model 3 is to be thought as an extreme example for the viscoelastic modelling and is probably not consistent with the actual viscosity below the Thuringian Slate Mountains. The buoyancy force, which is necessary for a viscoelastic investigation, is included after the approach introduced by Wu [2004].

6.4.2 Boundary conditions

The movement of the nodes in both models is constrained as follows:

(i) the nodes at the model bottom must not move in vertical direction (no slip);

(ii) the nodes at the vertical model boundaries must not move in horizontal direction perpendicular to the model sides (no slip).

These boundary conditions simulate the surrounding unmodelled Earth. It is assumed that the deformation signal of pressure changes at the earth surface decays with depth and over large horizontal distances. To ensure that the boundary conditions as well as the model size have no effect on the modelling results, we have carried out tests with different resolution, and found the used grid as appropriate for the model.

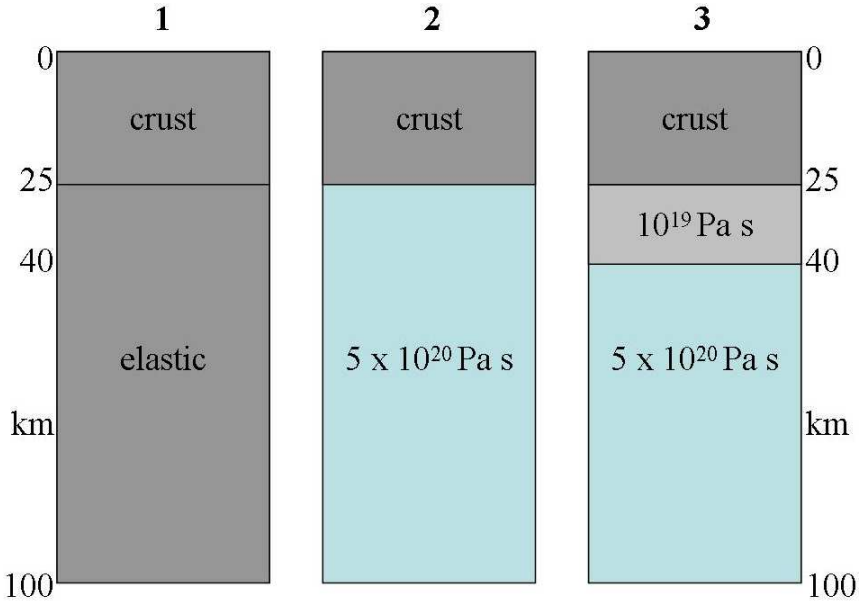

Figure 6.2: Structure of the three earth models.

6.4.3 Water load

The full water load of 182 Mill. m^3 is applied uniformly over the shape of the reservoir (Fig. 6.3), approximated by 135 element surfaces (250 m $\times$ 250 m), which correspond to a reservoir area of 8.44 km^2. The load is generated by dividing the water volume of the reservoir by this area multiplied with a water density of 1000 kg/m^3 and a gravity of 9.81 m/s^2. The full load of the Hohenwarte reservoir is 215,820 Pa corresponding to a constant water column of 22 m. The Eichicht reservoir has a full load of 58,860 Pa, a water column of 6 m.

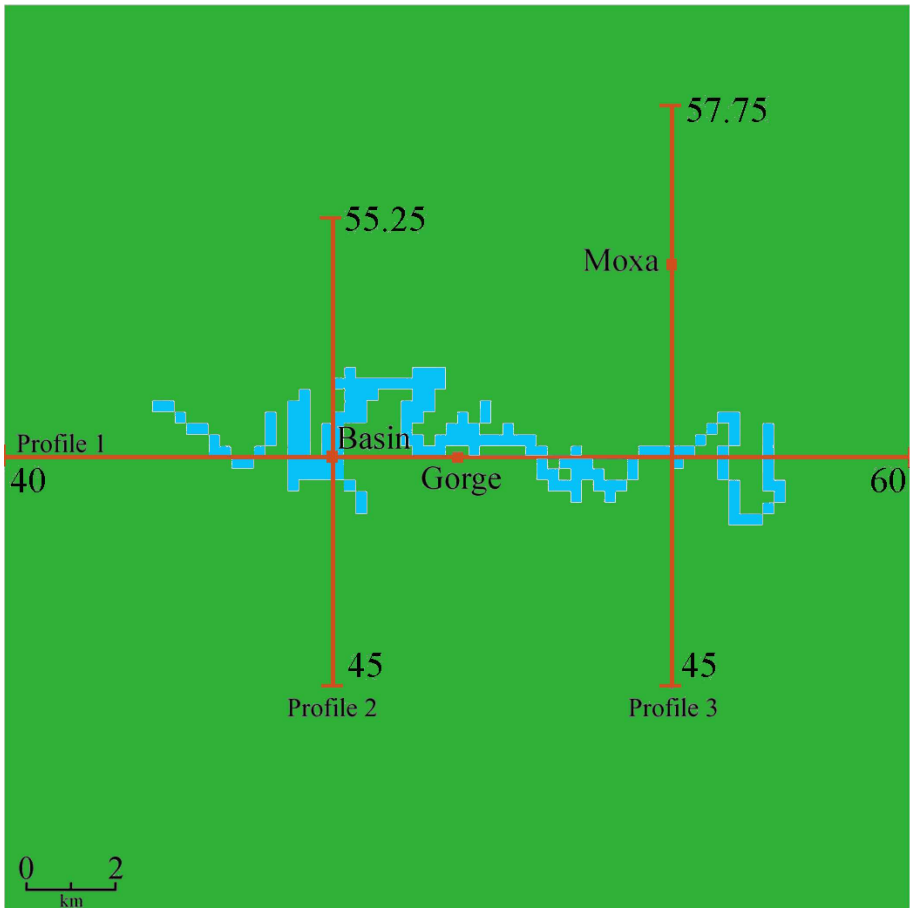

Figure 6.3: Top view of the model centre (20 km $\times$ 20 km) with the shape of the reservoir (white) and the profiles for the deformations. The location of the Geodynamic Observatory Moxa and the locations Basin and Gorge are marked. Numbers indicate locations in km relative to the entire grid of 100$\times$100 km used.

The load initially increases linearly over 2 years, after the dam was closed. Then, pressure changes simulating the seasons follow (Fig. 6.4). The filling starts at 0% of water volume in the year 1941 and ends after 2 years with a maximum water volume of 100%. In the next 6 months, the reservoir volume is reduced to 70% (summer) and after another 6 months increased again to 100% (winter). This cycle is repeated once. Thereafter the load is kept constant at 100% till the year 2011. With this approximation, we are able to study seasonal changes and we save computation time.

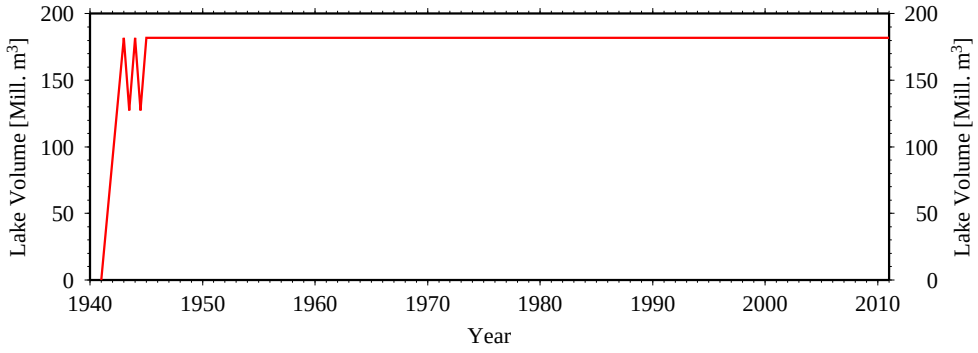

Figure 6.4: Lake volume as function of time.

6.5 Results

The deformation of the model by the time-dependent water load is calculated, and vertical deformations, strains and tilts are shown along three profiles (Fig. 6.3). Profile 1 starts west of the Eichicht reservoir and runs in EW–direction over the whole distance of the central frame. Profile 2 and 3 are directed perpendicular to Profile 1 from north to south. The location of Moxa observatory is at 54.25 km on Profile 3. The strain is obtained by calculating the difference of the horizontal displacements between two nodes and normalising this difference to the element length. The tilt is calculated as the angle resulting from the node displacement in EW– and NS–direction relative to the displacement of the next node vertically below (vertical tilt). This definition was successfully used for FE modellings by Fischer [2002], Kroner et al. [2005], and Steffen et al. [2006c]. In addition three points (Fig. 6.3) are selected to compare the vertical deformation on top of the model between the location in the greatest basin (Basin), in the centre of the model (Gorge) and at Moxa observatory (Moxa).

6.5.1 Short-term seasonal variations

Tilt: Fig. 6.5 shows the tilt in the NS– and EW–component for the elastic model (model 1) at different load times. To compare the results, the tilts at different times of an annual cycle are taken when the reservoir is filled-up (winter) and 70%-filled (summer). The tilt changes on each profile reflect the location of the reservoir and which reservoir border is tangent to the profile. The NS–component in Profile 1 shows for the southern border between 48 and 52 km a tilt northward and for the northern between 52 and 54 km a tilt southward. The tilt in the EW–component in Profile 1 traces the meanders of the old river valley. The tilts of Profile 2 are dominated by the load of the dam basin between 49 and 50.5 km. In Profile 3 the tilt only shows eye-catching changes when the reservoir is crossed at 50 km. The amplitude on all profiles is affected by the load sum in the vicinity of each point and is in winter at most 4.5 μrad eastward in the EW–component behind the dam. Between winter and summer significant differences in the amplitude of the tilts are found, especially at the location of the reservoir. Here, the tilt difference between winter and summer is at most 30% of the full load in winter and therefore a result of the elastic behaviour. Changes in the direction of the tilt are not observed.

The tilt changes of the viscoelastic models are not shown as there are only small differences in the tilts resulting from an elastic and a viscoelastic rheology. For example, the difference at the Basin and Gorge location is in the EW–component at most 0.2 nrad, in the NS–component at most 1 nrad. At Moxa

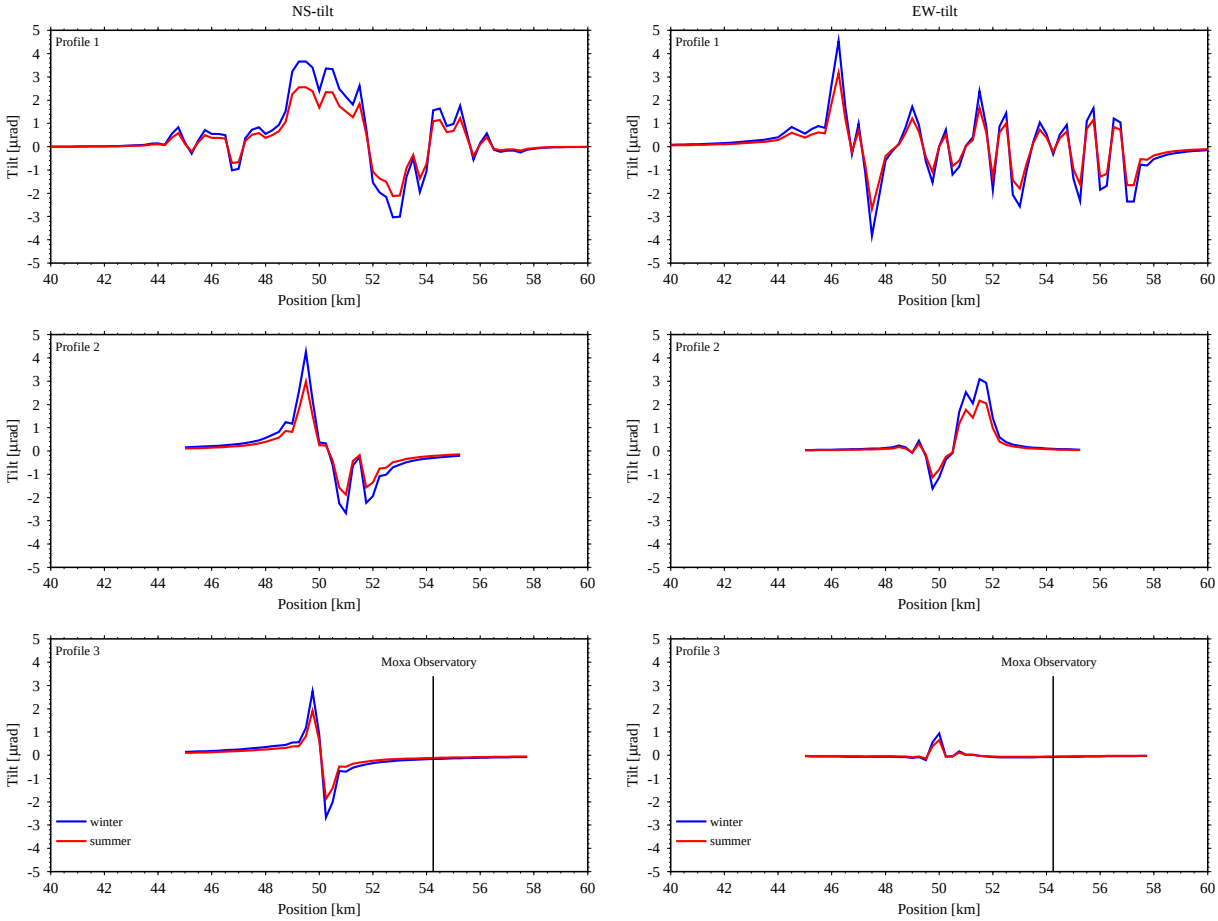

Figure 6.5: Tilt in the NS– component (left) and EW–component (right) obtained for the elastic model at different load times. Tilt northward and eastward positive.

location no difference is observed. The tilt differences are insignificant to the viscoelastic behaviour of the upper mantle for short-time load changes as they are too small for visible effects in tiltmeter registrations at Moxa. A comparison of the tilts in both components at Moxa location between different upper-mantle viscosities in the first mantle layer of 10^{19} Pa s (model 3) and 5 x 10^{20} Pa s (model 2) indicates 0.4 nrad larger effects for model 3.

Strain: Fig. 6.6 shows the strain in the NS– and EW–component for the elastic model at different load times, (1) when the reservoir is filled up (winter) and (2) 70%-filled (summer). The maximum amplitude is found in winter along Profiles 1 and 3 with around 1 μstrain compression. The strain changes reflect the location of the reservoir in compression. Profiles 2 and 3 demonstrate this behaviour clearly when the reservoir is crossed around 50 km. The extension observed in the EW–component of Profile 1 results between two meander valleys of the former river valley and is explained as compensation of the compression induced by the load in each valley. The amplitude is larger the more the valley distance increases and the less load is applied in vicinity of this point. As for the tilts, between winter and summer significant differences in the amplitude of the strains are found. At the location of the reservoir, the difference between winter and summer is at most 30% of the full load in winter and again a result of the elastic behaviour. No changes in the direction of the strain are detected.

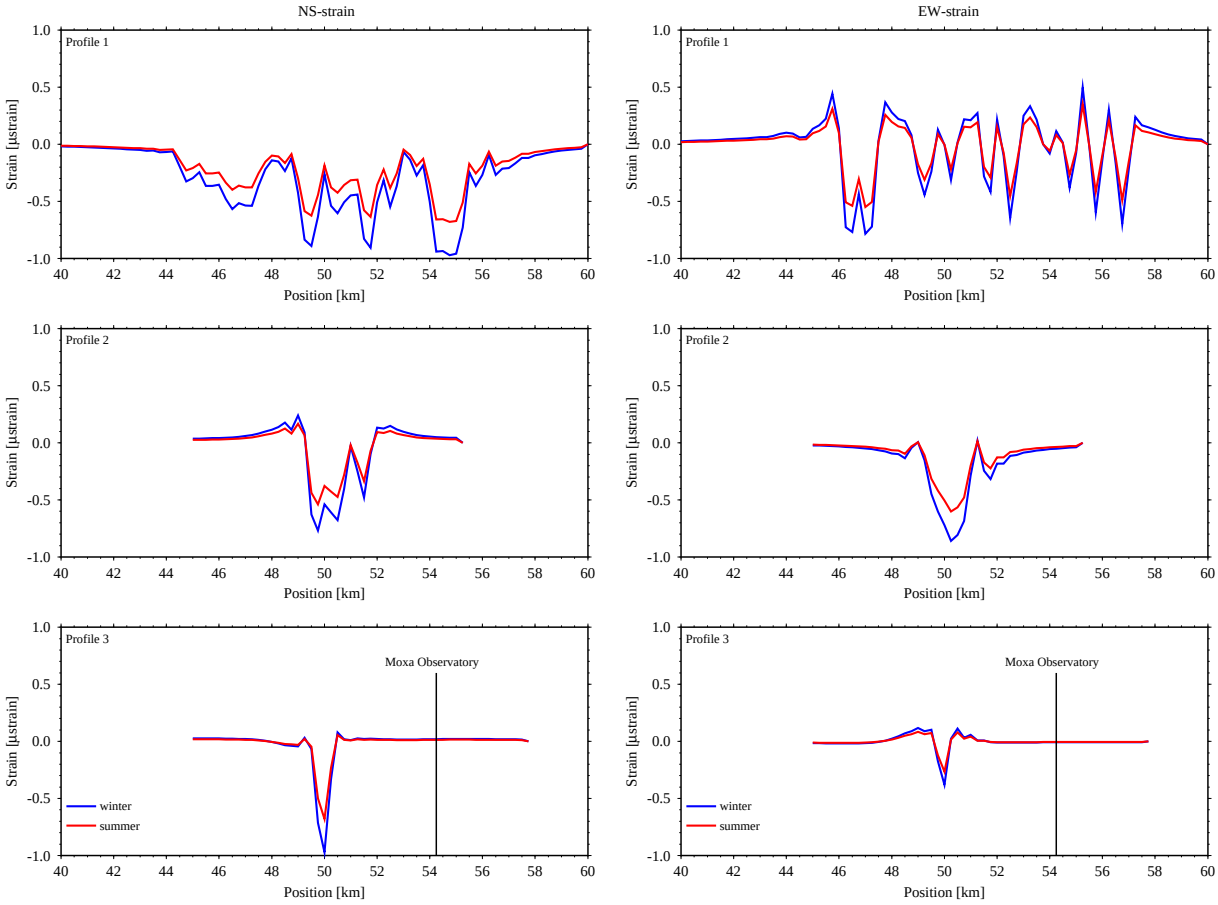

Figure 6.6: Strain in the NS–component (left) and the EW–component (right) obtained for the elastic model at different load times. Extension positive.

Again the strains resulting from a viscoelastic rheology are not shown, as the differences are to small to be seen. Existing, but small differences in the strains between an elastic and a viscoelastic rheology are found for both components at the location of the Basin and Moxa. At both locations this difference is at most 0.15 nstrain for both components when the reservoir is filled-up. For a 70%-filled reservoir in summer this effect is nearly doubled. The strains are as well as the tilts nearly independent of the viscoelastic behaviour of the upper mantle and the past load time. At the location of Moxa observatory, strain differences in the EW–component up to 0.2 nstrain between model 2 and 3 are found. At the Basin location 0.3 nstrain result.

Tilt and strain at Moxa: Fig. 6.7 shows for the location of the Moxa observatory the tilt and the strain in the NS– and EW–component for the elastic model in winter (filled-up) and summer (70%–filled). The maximum tilt in the EW–component is around 75 nrad westward and in the NS–component around 160 nrad southward. The maximum strain results for the EW–component in compression around 10 nstrain and for the NS–component in extension around 20 nstrain. The figure shows clearly the difference of 30% between winter and summer, which is at most 48 nrad in tilt and 6 nstrain in strain and should be observable with the sensitive instruments at Moxa [see Kroner et al., 2005, for a description]. In the tilt and the tilt direction to the source of pressure, which is applied around 50 km, a tendency to smaller effects is found. For the NS–component of the strain, which here results in extension, the curves

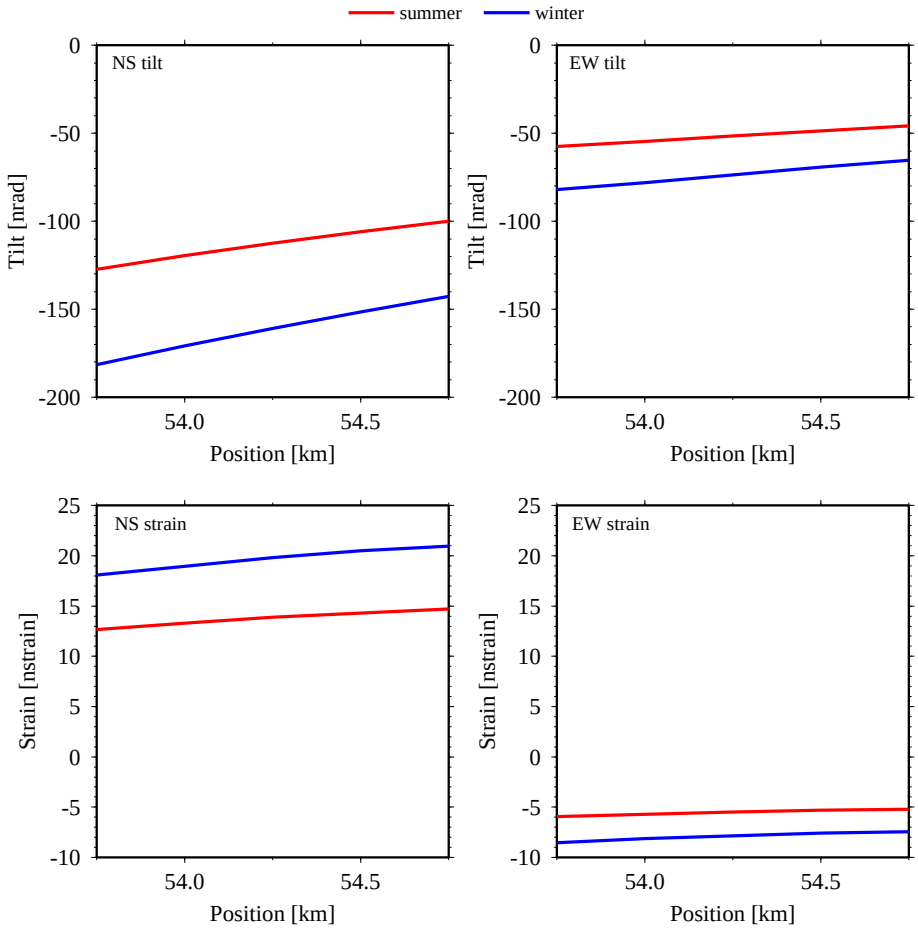

Figure 6.7: Tilts and strains in both components obtained for the elastic model at different load times at the location of Moxa observatory (54.25 km). Tilt eastward, northward positive. Extension positive.

diverge, which is explained as compensation for the compression at the location of the reservoir (see Fig. 6.6). As there are no significant differences in the strains and no differences in the tilts between an elastic and a viscoelastic rheology (see sections above), the curves for the viscoelastic models are not included.

6.5.2 Long-term seasonal variations

Vertical deformation: Fig. 6.8 shows the vertical deformation on the surface for all models at the three locations Basin, Gorge and Moxa for the load cycle. As expected, the greatest deformations are found near the dam (Basin) and the smallest in distance to the reservoir at the location of the observatory (Moxa). The curves reflect the location and the distance to the reservoir. The dominating elastic part (filled-up reservoir) at Moxa is about 0.85 mm, at the Gorge location 3.2 mm, and at the Basin location 5.1 mm. There is a clear difference between the results of the elastic model 1 and the viscoelastic model 3 after a long time period. The loading period of the Hohenwarte reservoir is sufficient for long-term deformation changes related to a viscosity of 10^{19} Pa s between 25 and 40 km depth, when a long time is taken into account. After 70 years, the viscoelastic part is responsible for 0.25 mm of vertical

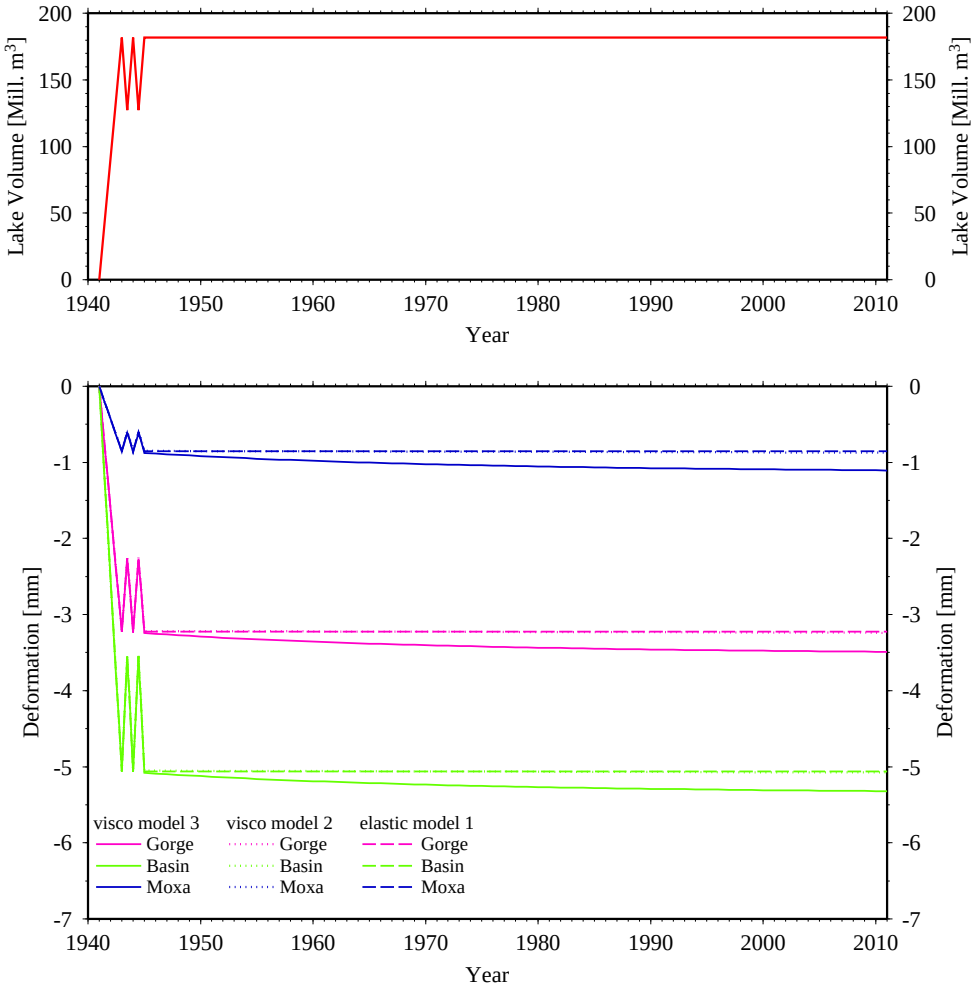

Figure 6.8: Top: Lake volume as a function of time. Bottom: Vertical deformation over 70 years obtained for all models at the three selected points Basin, Gorge and Moxa.

deformation. A comparison of the viscoelastic model 2 and the elastic model 1 shows nearly identical results. At Moxa the difference is about 5 μm after 4 years and about 17 μm after 70 years.

We have also investigated the effect of the Bleiloch reservoir, situated 10 km southeast of the observatory (Fig. 6.1). At the location of Moxa, an additional vertical deformation of 0.17 mm is induced, which, however, is spatially uniform at this location. Thus, the elastic deformation at Moxa will be around 20% larger, when the Bleiloch reservoir is also considered, but there is no significant effect in tilt and strain at the Moxa location. The remaining reservoirs have also no significant effect at the Moxa location, neither in tilt, strain or vertical deformation.

Differences in the vertical deformation induced by short-term load changes are mainly caused by the elastic crust. The viscoelastic part for viscoelastic model 3 is only around 6.2 μm, which corresponds to 2.4% of the deformation difference of 0.25 mm in 6 months. Regarding model 2, the viscoelastic part is in the range of 1 - 2 μm. Therefore, the short-term load change of the Hohenwarte-reservoir is not sensitive enough to observable vertical deformation induced by a upper mantle with a viscosity of 5×10^{20} Pa s or for the fictitious case of a upper mantle with a low-viscosity layer of 10^{19} Pa s.

Tilt and strain: The changes in the tilts and strains induced only by the viscoelastic relaxation are too small to be observed in registrations at Moxa observatory. Here, the viscoelastic part is for the strains around 2% of the elastic part of at most 20 nstrain, which is not observable in a time range of around 70 years. The tilts are not influenced.

6.6 Conclusions

Artificial reservoirs such as the Hohenwarte reservoir in Thuringia, Germany, induce additional loads on the Earth's surface. The resulting effects in tilt and strain deformations can be observed with sensitive instruments. In a distance of 4 km to the reservoir, where the Geodynamic Observatory Moxa is located, the influence of lake-level changes on the registrations is significant. It can be shown that the influence of lake-level fluctuations up to 30% to tilt and strain registrations at the observatory for all three different models is larger than the resolution of the instruments. At the location of Moxa differences of at most 48 nrad for the tilts and 6 nstrain for the strains are established. The vertical deformation is more affected by load changes. For the viscoelastic case the viscoelastic part is small compared to the elastic part and only observable over a long time period. For short-time lake-level fluctuations, the viscoelastic influence is less than 3%. All changes induced by lake-level fluctuations in the tilt, strain and vertical deformation should be observable at the Geodynamic Observatory Moxa independent of the model structure.

Acknowledgements

We are grateful for numerous comments and suggestions by Patrick Wu and an anonymous referee. This research was funded by the DFG (research grant KA1723/1-1).